International Journal of
Science and Engineering Investigations vol. 10, issue 113, June 2021
Received on June 26, 2021 ISSN: 2251-8843

The Performance of Hydrodynamic Journal Bearing Lubricated with Melon (Egusi) Seed and Coconut Seed Oils

Steven Odi-Owei[1], John Ameh[2], John Sodiki[3], Barinyima Nkoi[4]
[1,2,3,4]Department of Mechanical Engineering, Rivers State University, Nkpolu-Oroworukwo, Port Harcourt, Rivers State, Nigeria
([1]steveodiowei252@gmail.com, [2]Ikowad@yahoo.com, [3]jisodiki_partners@yahoo.com, [4]nkoi.barinyima@ust.edu.ng)

Abstract-This study investigated the effects of melon (citrullus lanatus) seed oil and coconut (cocos nucifera) seed oil on hydrodynamic journal bearing performance regarding pressure distribution, load carrying capacity and eccentricity ratio at varying loading and speed conditions. Vegetable oil-based lubricants are credible alternatives to petroleum based lubricants, which are not environmentally friendly. The melon seed oil and coconut seed oil were extracted using the Soxhlet extraction method, and then subjected to laboratory analyses. Journal bearing test apparatus was used to carry out the hydrodynamic pressure distribution and load capacity tests. The average hydrodynamic pressures generated with melon seed oil and coconut seed oil were, respectively, 21.56% and 6.28% lower than that of the SAE20W50 oil. Load carrying capacities were 24.45% and 6.97% lower while the eccentricity ratios were 96% and 103% higher, respectively. The experimental results were numerically validated. The overall performance of melon seed oil and coconut seed oil in this research confirmed that they are excellent candidate base oil stocks that should be fully exploited.

Keywords-*Melon Seed Oil, Coconut Seed Oil, Hydrodynamic Pressure, Load Carrying, Capacity, Eccentricity, Journal Bearing Apparatus*

I. INTRODUCTION

The industrial applications of lubrication are commonly found in rotating machines such as automotive engines, turbines, generators, pumps and compressors. These rotating machines are usually equipped with journal bearings, most especially hydrodynamic journal bearings. The hydrodynamic journal bearing is made up of the journal (shaft), which rotates in a casing (bearing). The lubricant oil is trapped in the clearance between the shaft and the casing. Adequate lubrication of hydrodynamic journal bearings minimizes friction and wear due to metal-to-metal contact, which mostly occurs during start and stop of the operations. Friction and wear are the major causes of power loss, material wastage and vibration in machinery. Thus, any means to reduce friction will lead to reduction of wear and its associated losses. Lubricants act as protective layers on surfaces of contacting bodies to minimize material loss (Yousif & El-Tayeb, 2008). Due to continuous motion of the shaft, hydrodynamic lubrication in journal bearings generates hydrodynamic pressure in the lubricant, and thus separates the shaft and the bearing surfaces from direct contact. The hydrodynamic pressure generated and the lifting force (load carrying capacity) on the shaft are two important performance measurements of the lubricated bearing. Here, the lubricant properties play significant roles in the overall hydrodynamic pressure distribution, load carrying capacity and the eccentricity ratio.

The influence of chemically modified rapeseed oil on tribological performance of journal bearings was investigated by Baskar et al. (2016) using the journal bearing test ring. The results of their experiment showed that copper dioxide nano-particle additives exhibited higher wear and friction reduction behaviour than the commercial synthetic lubricant oils. Similarly, Kumar and Gupta (2014) investigated the behaviour of hydrodynamic journal bearings under the influence of the multi-grade oil SAE 10W30. The experimental results were theoretically verified using Raimondi and Boyd charts and confirmed satisfactory. Khasbage et al. (2016) experimentally investigated the tribological properties of Jatropha oil and its performance in hydrodynamic journal bearings in comparison with the synthetic lubricant SAE40. The results showed that pure jatropha oil exhibited similar behaviour as the synthetic lubricant. Baskar and Sriram (2012) carried out an analysis of pressure distribution in a hydrodynamic journal bearings subjected to varying loading conditions and operating parameters under different vegetable oils such as rapeseed oil and soya bean oil. The results obtained were comparable with those of the commercial lubricant SAE20W40. Furthermore, pressure distribution and load carrying capacity of a hydrodynamic journal bearing were investigated using the Finite Element Method (FEM) and an analytical method by Nuruzzaman et al. (2010). Both results were in agreement with available published results, though numerical results were better; thus, confirming the validity of the study.

This study aimed at investigating the effects of Melon (citrullus lanatus) seed oil and Coconut (cocos nucifera) seed oil on hydrodynamic journal bearing performance regarding pressure distribution, load carrying capacity and eccentricity ratio at varying loading and speed conditions, with results compared with those obtained for the commercial engine oil SAE20W50.

II. MATERIALS AND METHODS

Five litres, each, of pure melon seed oil, coconut seed oil and SAE20W50 were used for each experiment as the apparatus' tank must be filled completely. The journal bearing used had a length of 0.0445m, a diameter of 0.0508m and a clearance of 0.000052m. Table 1 shows the physicochemical properties of the samples.

TABLE I. PHYSICOCHEMICAL PROPERTIES OF THE OIL SAMPLES

	Melon seed oil	Coconut seed oil	SAE20W50
Acid value (mg/g)	4.15	5.05	2.47
Peroxide value (mg/g)	0.80	0.20	0.20
Free fatty acid	2.08	2.53	1.23
Viscosity (cP)	99.09	72.67	420.00
Relative density	1.11	1.09	1.14
Saponification value (KOH/g)	46.28	93.97	-193.55

P5013 Journal Frictional Apparatus (including P5014-Pressure Distribution Apparatus) produced by Cussons Technology was used. The pressure distribution and the load-carrying capacities of the formulated lubricants and the reference oil (SAE20W50) were measured. The main journal friction apparatus was connected to a compressor for supply of compressed air maintaining a pressure of 6 bars (6x105 Pa). At the load of 490.5N, the speed of the motor was varied from 7, 5, 3, 2, to 1rev/sec, and at each speed, the pressure at the tapping points 1 to 5 along each of the axial holes A to F was measured. Similarly, at the speed of 5 rev/sec, the load on the bearing was varied from 98.1N through 196.2N, 294.3N, 392.4N to 490.5N and the pressure at each of the 5 tapping points, around the bearing surface, for each of the holes A to F was measured and recorded. The experimental set-up is shown in Fig. 1.

A. Analysis of Hydrodynamic Pressure and Load Carrying Capacity

The bearing casing (Fig. 1) was unwrapped into a rectangular shape and discretized into 6 x 5 elements. One-third of the circumference was used as shown in (1). Equation (2) represents the area of the unwrapped casing. The hydrodynamic force acting on the elements along axial hole A is expressed as (3) and the corresponding vertical force F_{Av} is expressed as (4) (Cussons Technology, 2015), for n=1, 2, 3, 4, 5.

$$B = \frac{\pi D}{3} \quad (1)$$

Where B = width of the unwrapped bearing sector; D = diameter of the bearing.

$$A = \frac{\pi D}{3} \quad (2)$$

where A = area of the unwrapped bearing sector; L = Length of the bearing.

$$F_A = A \sum_1^n P_{An} \quad (3)$$

where F_A = hydrodynamic forces along axial holes A, P_A = hydrodynamic pressures along axial holes A and n = number of axial holes from 1 to 5.

$$F_{Av} = A \sum_1^n P_{An} \cos\theta^0 \quad (4)$$

where F_{AV} = vertical component of hydrodynamic force (load carrying capacity) along axial hole A.

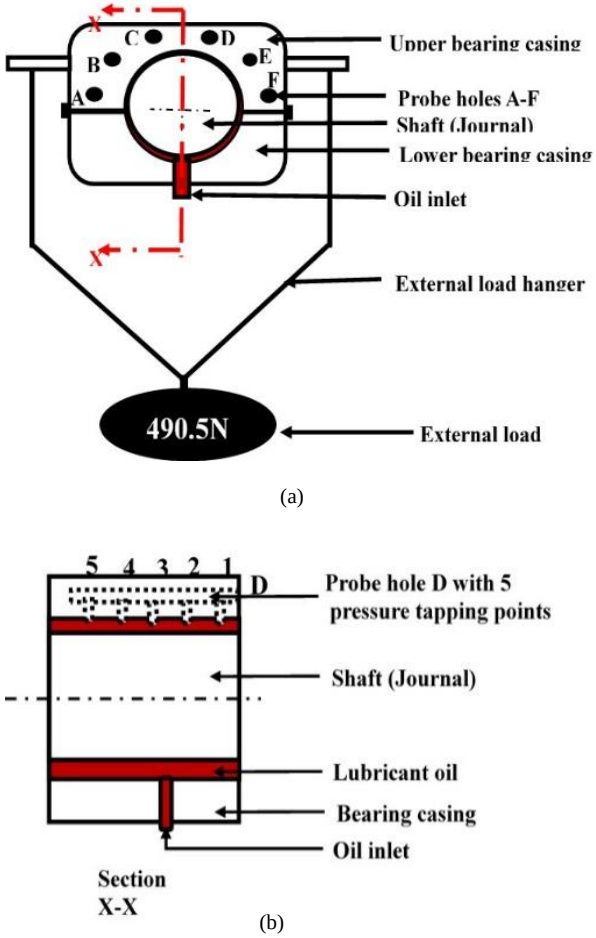

Figure 1. Schematic Drawing of Experimental Set-Up Showing (a) Journal Bearing Test Equipment, and (b) Sectional View X-X

The hydrodynamic pressure generated experimentally at each tapping points 1 to 5 along the axial holes A to F in Fig. 1a, is expressed as (5) while the hydrodynamic force is expressed as (6). The average pressure on the unwrapped plate was determined from (7).

$$P = \{\sum_1^n P_{An} + \sum_1^n P_{Bn} + \sum_1^n P_{Cn} + \sum_1^n P_{Dn} + \sum_1^n P_{En} + \sum_1^n P_{Fn}\} \quad (5)$$

where P = total hydrodynamic pressure, P_A-P_F = hydrodynamic pressures along axial holes A to F, respectively.

$$F = A\{\sum_1^n P_{An} + \sum_1^n P_{Bn} + \sum_1^n P_{Cn} + \sum_1^n P_{Dn} + \sum_1^n P_{En} + \sum_1^n P_{Fn}\} \quad (6)$$

where F = total hydrodynamic force along axial holes A to F.

$$P_{Average} = \frac{P}{\text{Total number of elements}} \quad (7)$$

where $P_{Average}$ = average hydrodynamic pressure across the bearing domain

B. Numerical Analysis

The relationship between the distribution of lubricant pressure as a function of speed and geometry of journal bearing, lubricant viscosity and oil clearance is analytically presented in Reynolds equation. For the practical application of Reynolds equation, a simplified 2-D form is used (Gundarneeya, 2015) and expressed as

$$\frac{\partial}{\partial x}\left(h^3 \frac{\partial p}{\partial x}\right) + \frac{\partial}{\partial y}\left(h^3 \frac{\partial p}{\partial y}\right) = 6U\eta \frac{dh}{dx} \quad (8)$$

where x = circumferential length of bearing along x-axis; y = axial length of bearing along y-axis

h = film thickness, P = hydrodynamic pressure separating the two sliding surfaces
U = sliding velocity in x-axis, ŋ = lubricant dynamic viscosity

$\frac{\partial}{\partial x}\left(h^3 \frac{\partial p}{\partial x}\right)$ = Flow term (poiseuille flow) due to pressure gradient in x-direction

$\frac{\partial}{\partial y}\left(h^3 \frac{\partial p}{\partial y}\right)$ = Flow term (poiseuille flow) due to pressure gradient in y-direction

$6U\eta \frac{dh}{dx}$ = Flow term (couette flow) due to fluid lubricant velocity in x-direction

Fig. 2 shows the basic geometry of a typical hydrodynamic journal bearing and key analytical features.

The Finite Element Method was used to numerically analyze the solutions to (8) by following procedural steps adopted by Nwosu (1998). The bearing in Fig. 2b was unwrapped and its surface was discretized into 50 by 50 bilinear rectangular-shaped finite elements as in Fig. 3. Fig. 3 has 1 node at each of the four corners of the rectangle. The interpolation function is linear within the rectangle in x and y directions (Fig. 3). The shape function for the element was developed from the interpolation function (Kwon and Bang, 1997; Khennane, 2013) for nodal pressure, P, as expressed.

in (9) or (10).

$$P = a_1 + a_2 x + a_3 y + a_4 \quad (9)$$

$$P = [1 \quad x \quad y \quad xy] \begin{Bmatrix} a_1 \\ a_2 \\ a_3 \\ a_4 \end{Bmatrix} \quad (10)$$

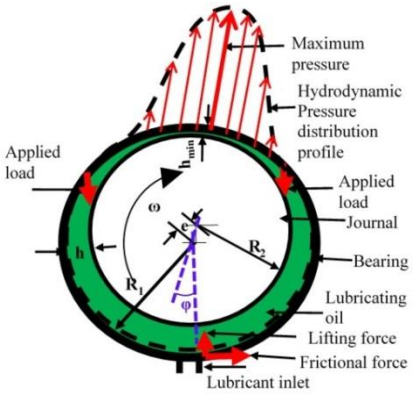

(a)

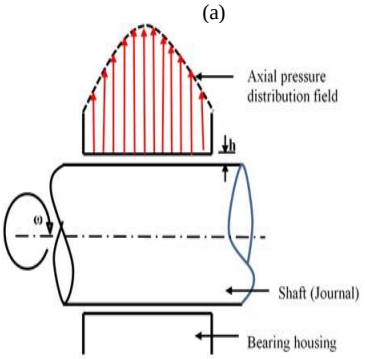

(b)

Figure 2. Journal Bearing Geometry: (a) Circumferential View, and (b) Axial View

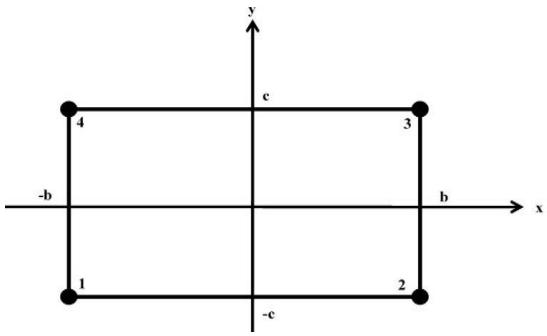

Figure 3. Bilinear Rectangular Element

Equation (11) considers four nodes of the element.

$$\begin{Bmatrix} p_1 \\ p_2 \\ p_3 \\ p_4 \end{Bmatrix} = \begin{bmatrix} 1 & x_1 & y_1 & x_1 y_1 \\ 1 & x_2 & y_2 & x_2 y_2 \\ 1 & x_3 & y_3 & x_3 y_3 \\ 1 & x_4 & y_4 & x_4 y_4 \end{bmatrix} \begin{Bmatrix} a_1 \\ a_2 \\ a_3 \\ a_4 \end{Bmatrix} \quad (11)$$

Substituting the coordinate values of Fig. 3 into (11) and following matrix algebra rules, we obtain

$$\begin{Bmatrix} a_1 \\ a_2 \\ a_3 \\ a_4 \end{Bmatrix} = \frac{1}{4bc}\begin{bmatrix} bc & bc & bc & bc \\ -c & c & c & -c \\ -b & -b & b & b \\ 1 & -1 & 1 & -1 \end{bmatrix}\begin{Bmatrix} p_1 \\ p_2 \\ p_3 \\ p_4 \end{Bmatrix} \quad (12)$$

Substituting (12) into (10) we obtain

$$P = \frac{1}{4bc}\begin{Bmatrix} (bc - cx - by + xy)p_1 + \\ (bc + cx - by - xy)p_2 \\ +(bc + cx + by + xy)p_3 + \\ (bc - cx + by - xy)p_4 \end{Bmatrix} \quad (13)$$

which can be represented as

$$P(x,y) = H_1(x,y)P_1 + H_2(x,y)P_2 + H_3(x,y)P_3 + H_4(x,y)P_4 \quad (14)$$

Equation (14) is the interpolation function for the 4-noded element of Fig. 3.

$H(x,y)$ is the Lagrange shape function for the bilinear rectangular element, which is expressed in (14a – 14d).

$$H_1 = \frac{1}{4bc}(b-x)(c-y) \quad (14a)$$

$$H_2 = \frac{1}{4bc}(b+x)(c-y) \quad (14b)$$

$$H_3 = \frac{1}{4bc}(b+x)(c+y) \quad (14c)$$

$$H_4 = \frac{1}{4bc}(b-x)(c+y) \quad (14d)$$

Equation 14 can be represented for ease of numerical computation as

$$P = \sum_{i=1}^{n} p_i H_i \quad (15)$$

Galerkin's method was used to convert the continuous partial differential equation (Reynolds equation) to a discrete algebraic equation by means of a weak formulation for the purpose of finding the solution numerically (Kwon and Bang, 1997). Equation (8) was multiplied by a test (weighted) function, W, and integrated by parts twice; first, with respect to x and second, with respect to y as shown in (16) to arrive at the weak formulation in (17).

$$I = \iint w\left[\frac{\partial}{\partial x}\left(h^3\frac{\partial p}{\partial x}\right) + \frac{\partial}{\partial y}\left(h^3\frac{\partial p}{\partial y}\right) - 6U\eta\frac{dh}{dx}\mathrm{dxdy}\right] \quad (16)$$

where I = weighted residual of Reynolds equation

$$I = -\int_\Omega h^3\left[\frac{\partial w}{\partial x}\frac{\partial p}{\partial x} + \frac{\partial w}{\partial y}\frac{\partial p}{\partial y}\right]d\Omega - \int_\Omega w\left[6U\eta\frac{dh}{dx}\right]d\Omega + \int_{\Gamma_n} h^3 w\frac{\partial p}{\partial n}d\Gamma = 0 \quad (17)$$

Solutions to (17) were obtained through numerical analysis using a MATLAB program. The first integral is a pressure term over the domain. The second integral is a velocity term due to wedge action of lubricant flow between the bearing and the journal surfaces while the line integral is a pressure term along the domain boundary where the pressure is considered zero. Substituting (17) into (15) and noting that, by Galerkin's method, weighting functions are identical with the shape functions (Wi = Hi) we obtain

$$\sum_{i=1}^{n} p_i \int_\Omega \frac{\partial H_i}{\partial x}\frac{\partial H_i}{\partial x}d\Omega + \sum_{i=1}^{n} p_i \int_\Omega \frac{\partial H_i}{\partial y}\frac{\partial H_i}{\partial y}d\Omega = -\frac{6U\eta}{h^3}\frac{dh}{dx}\int_\Omega H_i\, d\Omega \quad (18)$$

Rearranging in a matrix form (Erhunmwun & Akpobi, 2019) yields

$$[K^e]\{P_i\} = -\frac{6U\eta}{h^3}\frac{dh}{dx}\{F^e\} \quad (19)$$

where

$K^e = element\ pressure\ matrix$
$P_i = nodal\ pressure\ (4\ nodes\ per\ element)$ and $F^e = element\ velocity\ vector$

$$[K^e] = \int_{\Omega^e}\frac{\partial H_i}{\partial x}\frac{\partial H_i}{\partial x}d\Omega + \int_{\Omega^e}\frac{\partial H_i}{\partial y}\frac{\partial H_i}{\partial y}d\Omega \quad (20)$$

Substitute (14a-14d) into (20) to yields, for an element

$$K_{11}^e = \int_{-b}^{b}\int_{-c}^{c}\frac{1}{16b^2c^2}[(y-c)^2 + (x-b)^2]dydx \quad (21)$$

Wolfram Mathematica.9 software was used to compute the integral of elemental (21) to yield

$$K_{11}^e = \frac{c^2+b^2}{3bc} \quad (22)$$

Following the same integration procedure, the remaining elements in the element matrix were computed as

$$[K^e] = \begin{bmatrix} \frac{c^2+b^2}{3bc} & \frac{b^2-2c^2}{6bc} & \frac{b+c^2}{6bc} & \frac{c^2-2b^2}{6bc} \\ \frac{b^2-2c^2}{6bc} & \frac{c^2+b^2}{3bc} & \frac{c^2-2b^2}{6bc} & \frac{b+c^2}{6bc} \\ \frac{b+c^2}{6bc} & \frac{c^2+b^2}{3bc} & \frac{c^2+b^2}{3bc} & \frac{b^2-2c^2}{6bc} \\ \frac{c^2-2b^2}{6bc} & \frac{b+c^2}{6bc} & \frac{b^2-2c^2}{6bc} & \frac{c^2+b^2}{3bc} \end{bmatrix} \quad (23)$$

The same procedures were followed in the formulation of the element vector expressed as

$$F^e = \int_{\Omega^e} H_i\, d\Omega = \int_{-b}^{b}\int_{-c}^{c}\begin{Bmatrix} H_1 \\ H_2 \\ H_3 \\ H_4 \end{Bmatrix}dydx \quad (24)$$

With the aid of Mathematica application software, (24) was integrated to yield

$$F^e = \begin{Bmatrix} \frac{b^2c^2}{(b+x_0)(c+y_0)} \\ \frac{bc^2(b+2x_0)}{(b+x_0)(c+y_0)} \\ \frac{bc(b+2x_0)(c+2y_0)}{(b+x_0)(c+y_0)} \\ \frac{b^2c(c+2y_0)}{(b+x_0)(c+y_0)} \end{Bmatrix} \quad (25)$$

The following boundary conditions were used: P(x,0) = P(x,l) = 0, $\frac{dp}{dy}\Big|_{y=l/2} = 0$

III. RESULTS AND DISCUSSION

The results of the performance of the journal bearings in respect of the hydrodynamic pressure distribution, load-carrying capacity and the eccentricity are presented and discussed here:

A. Hdrodynamic Pressure Distribution

Figs. 4 and 5 show the hydrodynamic pressure performance of the plain journal bearing lubricated with coconut seed oil-based and melon seed oil-based stock as compared to the high-grade commercial engine oil (SAE20W50) under varying loading and angular speed conditions. In both cases, the results show similar trends where the generated hydrodynamic pressure increased with increase in angular speed of the journal and the externally applied load. These trends are in agreement with existing research literature (Srinivas et al., 2015). The maximum hydrodynamic pressure generated by SAE20W50 at maximum load was 0.86MPa while those for coconut seed oil and melon seed oil were 0.84MPa and 0.855MPa, respectively. Similarly, the maximum hydrodynamic pressure at the highest speed were 0.68MPa, 0.73MPa and 0.855MPa, respectively.

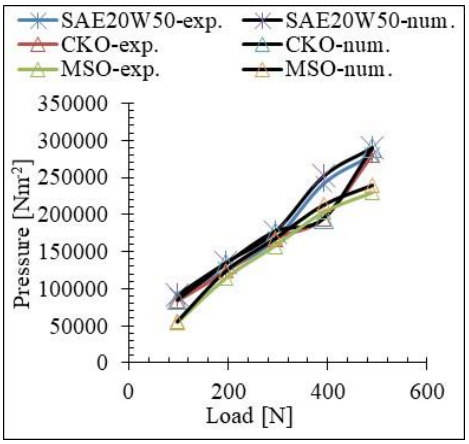

(a)

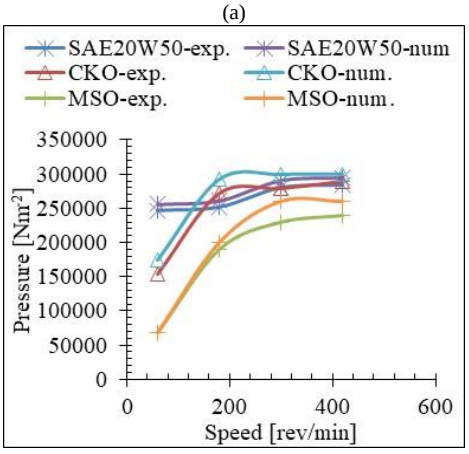

(b)

Figure 4. Hydrodynamic Pressure for Pure Coconut Seed Oil(CKO), Melon Seed Oil (MSO) and SAE20W50 Lubricants: (a) Against Load and (b) Against Speed

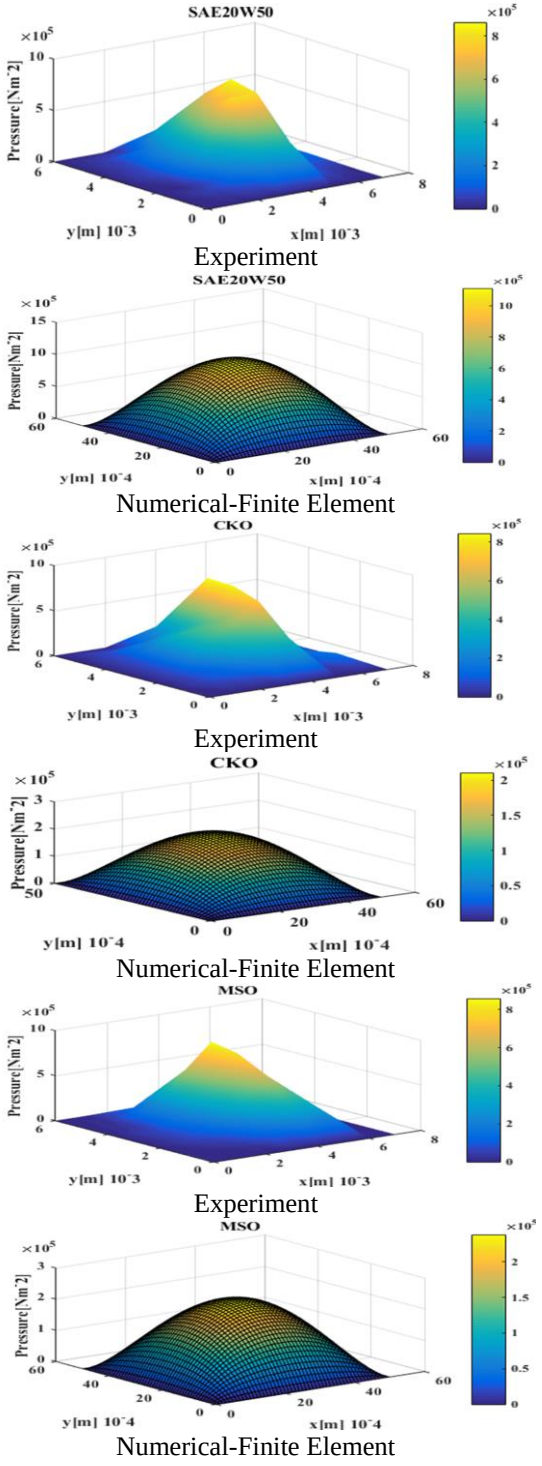

Figure 5. Hydrodynamic Pressure Distributions Profiles for Experimental and Numerical computation for SAE20W50 Lubricant, Coconut Seed oil (CKO) and Melon Seed Oil (MSO) at 420 rev/min

In both cases, coconut seed oil and melon seed oil, in their pure state, performed well as the high-grade reference commercial engine oil (SAE20W50).

B. *Load-Carrying Capacity*

Fig. 6 shows the dynamic load-carrying capacity performance of the hydrodynamic journal bearing, lubricated with pure coconut oil-based, melon seed oil-based stock and SAE20W50 lubricant. The trend in Fig. 6 shows that as the external load increased, the dynamic load-carrying capacity of the bearing also increased. A similar trend was shown with the increase in angular speed of the bearing.

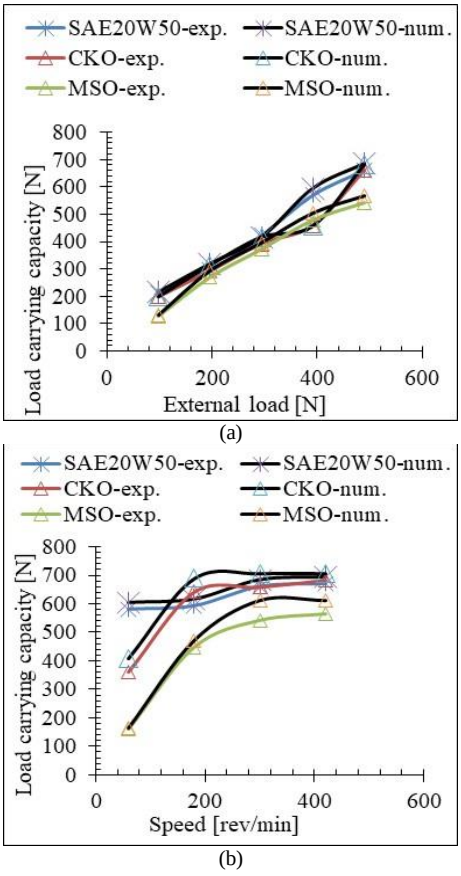

Figure 6. Load carrying Capacity for Pure Coconut Seed Oil (CKO), Melon Seed Oil (MSO) and SAE20W50 lubricants: (a) Against Load and (b) Against Speed

However, in both cases, the changes in external load had a more rapid change of the dynamic load carrying capacity. Both trends are in agreement with existing literature (Nuruzzaman et al., 2010). The total dynamic load carrying capacity was computed by integrating all the elemental nodal pressure contributions over the bearing surface area and multiplying the average pressure by the total surface area. At a constant external load of 490.5N and angular speed of 420rev/min, the maximum dynamic load carrying capacity of 0.669KN (SAE20W50), 0.683KN (coconut seed oil) and 0.564KN (melon seed oil) were computed from the experimental results.

C. *Effects of Eccentricity*

Fig. 7 shows graphs of angular speed and external load against eccentricity ratio for pure coconut seed oil-base, melon seed oil-base stock, and SAE20W50. The eccentricity ratio decreased with increase in the angular speed. The overall trend of the plotted results is in agreement with the published literature (Nuruzzaman et al., 2010).

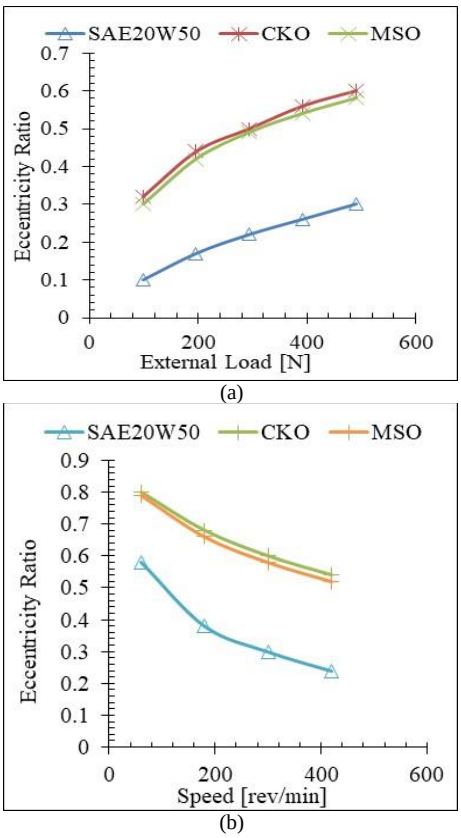

Figure 7. Eccentricity Ratio for Pure Coconut Seed Oil(CKO), Melon Seed Oil(MSO) and SAE20W50 Lubricants: (a) Against Load and (b) Against Speed

At the angular speed of 420rev/min and constant load of 490.5N, the eccentricity ratio was 0.24 (SAE20W50), 0.54 (coconut seed oil) and 0.62 (melon seed oil).

IV. CONCLUSION

This paper investigated the effects of melon seed oil and coconut seed oil on the performance of a hydrodynamic journal bearing. Hydrodynamic journal bearing tests were carried out under varying load and speed conditions, to determine the pressure distribution, load carrying capacity and the eccentricity ratio of pure coconut seed oil and melon seed oil. A commercial engine oil (SAE20W50) was used as control.

The overall results showed that the commercial engine oil (SAE20W50) performed slightly better than pure coconut seed oil and pure melon seed oil. In all cases, the generated hydrodynamic pressure increased with increase in external load (at constant speed) and with increase in speed (at constant external load). In the same way, load-carrying capacity increased with increase in speed, and increase in external load.

The shaft eccentricity decreased with increase in speed (at constant external load) and increased with increase in external load (at constant speed). The performance of pure coconut seed oil and melon seed oil were comparable to that of the high grade commercial engine oil (SAE20W50). The experimental results were validated with numerical analysis using the finite element method. Melon seed oil and coconut seed oil have great potential as excellent lubricant oil-based stock.

ACKNOLOWDGMENTS

The authors would like to acknowledge Prof. F. O. Anafi, the Head of the Department of Mechanical Engineering, Ahmadu Bello University, Zaria, who authorized the use of the laboratory equipment, Rev. D. Yusuf, the Chief Technologist and Malam T. K. Bashir, the Technician, and all their support personnel for their assistance and encouragement in ensuring the completion of the laboratory experiments.

REFERENCES

[1] Baskar, S., Sriram, G., & Arumugam, S. (2016). Tribological Analysis of a Hydrodynamic Journal Bearing under the Influence of Synthetic and Biolubricants. *Tribology Transactions, 60(3), 428–436.*

[2] Baskar, S., & Sriram, G. (2012). Experimental Analysis of Hydrodynamic Journal Bearing Under Different Biolubricants. *IEEE-International Conference On Advances in Engineering, Science and Management (ICAESM -2012)*, 132-135, Nagapattinam.

[3] Cussons Technology (2015). P5013 Journal Friction Apparatus Including P5014 Pressure Distribution Apparatus and P5015 Bearing Attitude Apparatus, Issue 6.

[4] Erhunmwun, I. D & Akpobi, J. A. (2019). Pressure Distribution of Fluid in a Journal Bearing Considering the Effect of Side or End Leakage, Using the Two Dimensional Reynolds Model. *The International Journal of Materials and Engineering Technology*, 2(1), 8-15.

[5] Gundarneeya, T. P. (2015). Theoretical Analysis of Journal Bearing with Nanolubricants. *International Journal of Scientific Research in Science, Engineering and Technology*, 1(3),365-371.

[6] Khasbage, S., Patil, V., & Dhande, D. (2016). Performance of Jatropha Biolubricant for Hydrodynamic Journal Bearing Lubrication. *International Research Journal of Engineering and Technology*, 3 (7), 627-632.

[7] Khennane, A. (2013). Introduction to Finite Element Analysis Using MATLAB and Abaqus.New York, NY: CRC Press.

[8] Kumar, P., & Gupta, A. K. (2014). Experimental Investigation on Hydrodynamic Journal Bearing Using SAE 10W30 Multi Grade Oil. *International Journal of Advance Research and Innovation*, 2 (1), 166-173.

[9] Kwon, Y. W. & Bang, H. (1997) The Finite Element Method Using MATLAB. Washington DC: CRC Press.

[10] Nuruzzaman, D. M., Khalil, M. K., Chowdhury, M. A., & Rahaman, M. L. (2010). Study on Pressure Distribution and Load Capacity of a Journal Bearing Using Finite Element Method and Analytical Method. *International Journal of Mechanical & Mechatronics Engineering*, 10 (5), 1-8.

[11] Nwosu, H. U. (1998). Basic Finite Element Structural Analysis. Owerri: Readon Publishers.

[12] Srinivas, Yunus, M., Munshi, S. M., & Hussain, I. H. (2015). Performance Evaluation of Hydrodynamic Journal Bearing Using Gearbox and Engine Oil (SAE90 and SAE20w50) by Experimental and Theoretical Methods. *International Journal of Mechanical Engineering and Information Technology*, 3 (11), 1573-1583.

[13] Yousif, B. F., & El-Tayeb, N. S. M. (2008). Wear and Friction Characteristics of CGRP Composite Under Wet Contact Condition Using Two Different Test Techniques. *Wear*, 265 (5-6), 856-864.

How to Cite this Article:

Odi-Owei, S., Ameh, J., Sodiki, J. & Nkoi, B. (2021). The Performance of Hydrodynamic Journal Bearing Lubricated with Melon (Egusi) Seed and Coconut Seed Oils. International Journal of Science and Engineering Investigations (IJSEI), 10(113), 61-67. http://www.ijsei.com/papers/ijsei-1011321-09.pdf